THE JOURNAL OF BIOLOGICAL CHEMISTRY VOL. 287, NO. 36, pp. 30063–30072, August 31, 2012

The E3 Ubiquitin Ligase Protein Associated with Myc (Pam) Regulates Mammalian/Mechanistic Target of Rapamycin Complex 1 (mTORC1) Signaling *in Vivo* through N- and C-terminal Domains*

Received for publication, February 16, 2012, and in revised form, July 13, 2012 Published, JBC Papers in Press, July 13, 2012, DOI 10.1074/jbc.M112.353987

Sangyeul Han[‡1], **Sun Kim**[‡], **Samira Bahl**[‡2], **Lin Li**[‡2], **Clara F. Burande**[‡], **Nicole Smith**[‡], **Marianne James**[‡], **Roberta L. Beauchamp**[‡], **Pradeep Bhide**[§], **Aaron DiAntonio**[¶], **and Vijaya Ramesh**[‡3]

From the [‡]*Center for Human Genetic Research and* [§]*Department of Neurology, Massachusetts General Hospital, Boston, Massachusetts 02114 and the* [¶]*Department of Molecular Biology and Pharmacology, Washington University, St. Louis, Missouri 63110*

Background: Pam and its homologs act as key regulators of axon guidance and outgrowth and synapse development.
Results: Pam regulates mTORC1 signaling *in vivo*, and attenuated mTORC1 signaling may partly explain the axonal defects in *Phr1*-deficient mice.
Conclusion: mTORC1-dependent and -independent mechanisms contribute to neurodevelopmental defects in *Phr1* deficiency.
Significance: Understanding how Pam regulates synapse development will have direct relevance for diverse aspects of neural development.

Pam and its homologs (the PHR protein family) are large E3 ubiquitin ligases that function to regulate synapse formation and growth in mammals, zebrafish, *Drosophila*, and *Caenorhabditis elegans*. *Phr1*-deficient mouse models (*Phr1*$^{\Delta 8,9}$ and *Phr1*^{Magellan}, with deletions in the N-terminal putative guanine exchange factor region and the C-terminal ubiquitin ligase region, respectively) exhibit axon guidance/outgrowth defects and striking defects of major axon tracts in the CNS. Our earlier studies identified Pam to be associated with tuberous sclerosis complex (TSC) proteins, ubiquitinating TSC2 and regulating mammalian/mechanistic target of rapamycin (mTOR) signaling. Here, we examine the potential involvement of the TSC/mTOR complex 1(mTORC1) signaling pathway in *Phr1*-deficient mouse models. We observed attenuation of mTORC1 signaling in the brains of both *Phr1*$^{\Delta 8,9}$ and *Phr1*^{Magellan} mouse models. Our results establish that Pam regulates TSC/mTOR signaling *in vitro* and *in vivo* through two distinct domains. To further address whether Pam regulates mTORC1 through two functionally independent domains, we undertook heterozygous mutant crossing between *Phr1*$^{\Delta 8,9}$ and *Phr1*^{Magellan} mice to generate a compound heterozygous model to determine whether these two domains can complement each other. mTORC1 signaling was not attenuated in the brains of double mutants (*Phr1*$^{\Delta 8,9/Mag}$), confirming that Pam displays dual regulation of the mTORC1 pathway through two functional domains. Our results also suggest that although dysregulation of mTORC1 signaling may be responsible for the corpus callosum defects, other neurodevelopmental defects observed with *Phr1* deficiency are independent of mTORC1 signaling. The ubiquitin ligase complex containing Pam-Fbxo45 likely targets additional synaptic and axonal proteins, which may explain the overlapping neurodevelopmental defects observed in *Phr1* and *Fbxo45* deficiency.

Tuberous sclerosis complex (TSC),[4] in which slow growing, benign hamartomas form in multiple organs, is caused by mutations in tumor suppressor genes encoding hamartin (*TSC1*) and tuberin (*TSC2*), respectively. TSC-associated CNS defects, including seizures and mental retardation, and features of autism spectrum disorder are present in 30–60% of individuals with TSC (1). The TSC1-TSC2 protein complex functions as a critical negative regulator of mammalian/mechanistic target of rapamycin (mTOR) complex 1 (mTORC1)-mediated signaling. The TSC proteins act as a central hub relaying signals from diverse cellular pathways to control mTORC1 activity (2, 3). mTORC1 signaling plays an important role in neurodevelopment by modulating both general and neuronal activity-dependent protein synthesis. More importantly, long-lasting forms of synaptic plasticity and memory are dependent on new protein synthesis, and aberrant mTORC1 signaling is reported in many neurological disorders (4–6).

* This work was supported, in whole or in part, by National Institutes of Health Grants NS024279 (to V. R.) and DA020812 (to A. D.). This work was also supported by a grant from Autism Speaks, Simons Foundation for Autism Research Initiative (to V. R.), and a fellowship from the Tuberous Sclerosis Alliance (to S. B.).

[1] Present Address: Bio Lab, Samsung Advanced Institute of Technology, Yongin, Gyeonggi 446-712, Korea.
[2] Both authors contributed equally to this work.
[3] To whom correspondence should be addressed: Center for Human Genetic Research, Massachusetts General Hospital, Richard B. Simches Research Bldg., 185 Cambridge St., Boston, MA 02114. Tel.: 617-724-9733; Fax: 617-643-3203; E-mail: ramesh@helix.mgh.harvard.edu.

[4] The abbreviations used are: TSC, tuberous sclerosis complex; mTOR, mammalian/mechanistic target of rapamycin; mTORC1, mTOR complex 1; Pam, protein associated with Myc; RCC, regulator of chromosome condensation; RHD, RCC homology domain; GEF, guanine exchange factor; RZF, RING zinc finger; Ub, ubiquitin; DLK, dual-leucine zipper kinase; S6K, S6 kinase; E, embryonic day; GTPγS, guanosine 5′-3-*O*-(γ-thio)triphosphate.

We previously identified protein associated with Myc (Pam) as a TSC2 interactor and demonstrated a genetic interaction between the homologs of these proteins in *Drosophila* (7). Human Pam belongs to an evolutionally conserved family of large proteins (PHR family), including Phr1 (for Pam/Highwire/RPM-1) in mouse, Highwire (HIW) in *Drosophila*, RPM-1 (regulator of presynaptic morphology 1) in *Caenorhabditis elegans*, and Esrom in zebrafish, and all family members encode >80 exons averaging about 4000 amino acids. These proteins contain multiple conserved motifs, which include regulator of chromosome condensation (RCC) homology domains (RHD-1 and RHD-2) with inferred guanine exchange factor (GEF) activity, a Myc-binding domain, a B-box zinc finger, and a C-terminal RING zinc finger (RZF) domain, which is a hallmark motif for E3 ubiquitin (Ub) ligase activity (8–10). Several genetic studies demonstrated that Pam homologs regulate presynaptic growth and development (11–15). Members of the PHR family have been suggested to control a variety of signaling pathways, including JNK/p38 MAPK signaling in *Drosophila* and *C. elegans* (16–18), bone morphogenetic protein signaling in *Drosophila* (19), and cAMP signaling in mammalian cells (20). In addition, RPM-1 positively regulates a Rab GTPase pathway to promote vesicular trafficking via late endosomes, thereby regulating synapse formation and axon termination (21). Results obtained from both *Drosophila* and *C. elegans* suggest that the highly conserved RZF domain is critical for the E3 Ub ligase activity of Pam homologs, particularly for the regulation of synapse development (16, 17, 22). Our previous work demonstrated that Pam interacts with specific E2 enzymes and is capable of ubiquitinating TSC2; furthermore, suppression of Pam in primary dissociated neurons results in stabilization of TSC2 and down-regulation of mTORC1 signaling (23). Because Ub and ubiquitination enzymes have emerged as key regulators of synapse development, function, and plasticity (24, 25), our findings suggested that Pam, as an E3 Ub ligase and a regulator of TSC/mTOR signaling, could play an essential role in neuronal activity-dependent protein synthesis and synapse development and function in mammalian neurons.

Phr1 mouse models generated in recent years demonstrate the importance of Phr1 in axon guidance and outgrowth and synapse development. In an *N*-ethyl-*N*-nitrosourea-induced genetic screen for morphological defects in mouse embryonic motor neurons, mutants harboring a premature stop codon in exon 63 of *Phr1* were isolated and named *Magellan* (referred to here as $Phr1^{Mag}$). The *Phr1* gene contains ~86 exons, and a premature stop codon in exon 63 of the $Phr1^{Mag}$ allele results in deletion of the C-terminal region of Pam containing the E3 Ub ligase domain. However, a truncated N-terminal segment of the protein encompassing the RHD region (putative GEF) is stably expressed in these mutants (26). In the genetically engineered model of *Phr1* described by Bloom *et al.* (27), exons 8 and 9, encoding 70 amino acids adjacent to the highly conserved RHD, are deleted in-frame either conditionally in selected regions of the brain or constitutively in all organs. In this $Phr1^{\Delta 8,9}$ model, the C-terminal E3 Ub ligase motif is intact. These mouse models are valuable in understanding the functions of N- and C-terminal motifs, the RHD (putative GEF function) and the RZF (E3 Ub ligase activity), respectively.

Employing these models, we show here that mTORC1 signaling is compromised in the brains of both $Phr1^{Mag}$ and $Phr1^{\Delta 8,9}$ models; however, the TSC1-TSC2 complex is stabilized only in $Phr1^{Mag}$ mice and not in $Phr1^{\Delta 8,9}$ mice. In addition, we generated a compound heterozygous model ($Phr1^{\Delta 8,9/Mag}$) that demonstrates complementation of each domain with respect to mTORC1 signaling. Collectively, our results provide both *in vitro* and *in vivo* evidence that Pam/Phr1 regulates mTORC1 signaling through two functionally independent domains. We also provide *in vivo* evidence that thinning of the corpus callosum reported in *Phr1*-deficient mice may be due to down-regulation of mTORC1 signaling.

EXPERIMENTAL PROCEDURES

Antibodies and Reagents—All antibodies were purchased from Cell Signaling Technology, with the exception of anti-α-tubulin and anti-FLAG antibodies (Sigma), anti-HA antibody (Covance), anti-Myc antibody (clone 9E10, Developmental Studies Hybridoma Bank, University of Iowa), anti-actin and anti-GAPDH antibodies (Santa Cruz Biotechnology), anti-Rheb (Ras homology enriched in brain) and anti-MYCBP2 (ab86078) antibodies (Abcam), anti-dual-leucine zipper kinase (DLK) antibody (Dr. Lawrence Holzman, University of Michigan Medical School), anti-Fbxo45 antibody (Dr. Hideyuki Okano, Keio University, Tokyo, Japan), and anti-TSC1 antibody (28). Affinity-purified PF3, an anti-Pam/Phr1 rabbit polyclonal antibody, was generated in our laboratory against a maltose-binding protein-Pam fusion protein (amino acids 1–150). The Rheb shRNA clone was purchased from Open Biosystems. Stimulation experiments were performed using insulin (Sigma). Rapamycin was purchased from Calbiochem. The Myc-Rheb overexpression plasmid was a kind gift from Dr. Kun-Liang Guan (University of California, San Diego, CA), and Myc-tagged PamF1 and PamF3 plasmids were described previously (29). Lipofectamine 2000, Lipofectamine, and PLUS reagent were purchased from Invitrogen.

Phr1 Mouse Models and Genotyping—$Phr1^{Mag}$ stock mice were obtained from Dr. Samuel L. Pfaff (Salk Institute for Biological Studies, La Jolla, CA) (26), and conventional $Phr1^{\Delta 8,9}$ stock mice have been described previously (27). To generate compound heterozygous $Phr1^{\Delta 8,9/Mag}$ mice, heterozygous $Phr1^{\Delta 8,9/+}$ mice were crossed with heterozygous $Phr1^{Mag/+}$ mice. Day 18.5 embryos were collected from timed pregnant matings. All genotyping was performed by PCR analysis using genomic DNA isolated from ear punch or tail samples. For $Phr1^{\Delta 8,9}$ mutant mice, the presence of the WT allele or mutant allele was verified as described previously (27). $Phr1^{Mag}$ mutant mice were genotyped using PCR methods, followed by restriction enzyme digestion using Hpy8I (Fermentas) to separate the WT and mutant alleles as described (26). Genotyping of the compound heterozygous $Phr1^{\Delta 8,9/Mag}$ mouse model utilized methods for both $Phr1^{\Delta 8,9}$ and $Phr1^{Mag}$ mice.

Standard and Real-time RT-PCR—Total RNA was isolated using the RNeasy minikit (Qiagen) according to the manufacturer's instructions. First-strand cDNA was generated using SuperScript™ II reverse transcriptase (Invitrogen) according to the manufacturer's instructions. RT-PCR for *Phr1* was carried out employing two sets of mouse-specific primers: the

5′-*Phr1* (exon 3) primer GCTGCATCGAAAAACTCAGTACA and the 3′-*Phr1* (exon 3/4) primer CCCAACCTCAATAATCTTTGGCA, as well as the 5′-*Phr1* (exon 71) primer TGAAGGAACACATGGTTGGA and the 3′-*Phr1* (exon 72) primer GATATGGCGTGTTCCCATTC. Real-time RT-PCR was performed in triplicate using the Roche LightCycler® 480 system. Mouse-specific primers were designed using the web-based program Primer3 (Version 4.0). Primers included the 5′-*Fbxo45* primer GCTGGAATCTGGTGGACAAT and the 3′-*Fbxo45* primer CCCACGCTCAAAAGCTAAAG. Reactions were performed using iTaq™ SYBR® Green Supermix with ROX (Bio-Rad). Acquired data were analyzed using LightCycler® 480 software. Gene expression levels were normalized to *Gapdh*. As a control for standard and real-time RT-PCR, mouse-specific *Gapdh* primers (5′-AGGTCGGTGTGAACGGATTTG and 3′-TGTAGACCATGTAGTTGAGGTCA) were utilized.

Cell Culture, Transfection, Transduction, and Western Blotting—HEK293T cells were maintained in high glucose DMEM (Invitrogen) containing 10% fetal bovine serum (Sigma). For overexpression of HA-S6 kinase (S6K), Myc-Rheb, Myc-PamF1, and Myc-PamF3 constructs, HEK293T cells were transfected using Lipofectamine 2000 as recommended by the manufacturer. For Rheb RNAi experiments, 1 day prior to transfection, lentivirus expressing either Rheb shRNA or a nontargeting scrambled control was transduced into HEK293T cells, followed by transfection of HA-S6K alone or with Myc-PamF1 using Lipofectamine and PLUS reagent according to the manufacturer's recommendations. For serum-deprived conditions, 18–20 h after transfection, cells were serum-deprived for 24 h, followed by immunoblot analysis. For insulin-stimulated conditions, following 24 h of serum deprivation, cells were stimulated for 30 min using a final dilution of 1 μl/ml insulin. Amino acid depletion experiments and rapamycin treatment were performed as described (30). All lysates from mouse tissues or cultured cells were prepared in either 0.5% Nonidet P-40 lysis buffer or standard radioimmune precipitation assay buffer containing 1× Halt™ phosphatase inhibitor mixture (Thermo Scientific) and 1× Complete protease inhibitor mixture (Roche Applied Science). For S6K immunoprecipitation, protein lysates (500 μg) were incubated with 2–3 μg of primary antibody for 15 h at 4 °C, mixed with protein A-Sepharose, and incubated for 3 h. Immunoprecipitates or protein lysates were separated by 4–15% gradient SDS-PAGE (Bio-Rad) and detected with primary antibodies as indicated. For quantification of immunoblotting data, bands were scanned, and intensities were calculated by densitometry (Bio-Rad). Western blotting for endogenous Pam/Phr1 was carried out on whole brain lysates from $Phr1^{Mag}$ and $Phr1^{\Delta 8,9}$ mice (embryonic day (E) 17.5) using NuPAGE 3–8% Tris acetate gels (Invitrogen) as described previously (26). Statistical analysis of scanned images was determined using Student's two-tailed *t* test.

Histology—Whole mount brains from E18.5 mice were processed by either coronal cryosectioning methods as described previously (27) with minor modifications or by fixation in Bouin's solution (Sigma), followed by coronal paraffin sectioning. Briefly, for cryosectioning, whole brains were fixed in 4% paraformaldehyde, cryoprotected by serially transferring to 15 and 30% sucrose solutions, sectioned at 20-μm thickness, and stained with a solution of 0.1% aqueous cresyl violet acetate (Sigma). For paraffin sectioning, whole embryos were fixed for 24 h and then washed with 70% ethanol, followed by 6-μm step sectioning and hematoxylin and eosin staining. Paraffin sectioning procedures, including embedding, step sectioning, staining, and analysis, were carried out by the Rodent Histopathology Core at the Dana Farber/Harvard Cancer Center (Boston, MA).

RESULTS

Compromised mTORC1 Signaling in Phr1 Mutant Mice—We reported previously that suppression of Pam by RNAi in dissociated neurons results in increased TSC2 levels and down-regulation of mTORC1 signaling, supporting the hypothesis that Pam may act as an E3 Ub ligase for TSC2 (23). To test the *in vivo* role of Pam in TSC/mTOR signaling, we examined two mouse models of Pam, $Phr1^{Mag}$, in which the C-terminal RZF domain with the E3 Ub ligase activity is deleted (26), and $Phr1^{\Delta 8,9}$, with an intact C-terminal RZF motif (27) (Fig. 1*A*). We observed a reduction of phosphorylation of downstream mTORC1 targets, including S6K (S6K phosphorylated at Thr-389) and S6 (S6 phosphorylated at Ser-240/Ser-244 and Ser-235/Ser-236), in brain lysates of both homozygous mutant models. To our surprise, the down-regulation of phospho-S6K and phospho-S6 was more significant in $Phr1^{\Delta 8,9}$ mice, in which the RZF domain is intact, compared with $Phr1^{Mag}$ mice, with the deleted RZF domain (Fig. 1, *B* and *C*). The levels of S6K and S6 phosphorylation in brain lysates from both heterozygous mouse models were indistinguishable from those from WT mice. We did not observe any change in phosphorylation of 4E-BP1, another downstream target of mTORC1 signaling in either model, suggesting a differential regulation of this effector protein. We also did not see any change in phosphorylation of Akt and ERK. The compromised mTORC1 signaling was not seen in other embryonic tissues from $Phr1^{Mag}$ and $Phr1^{\Delta 8,9}$ mouse models, suggesting that Pam regulation of mTORC1 signaling may be restricted to the brain (data not shown).

Employing standard and real-time RT-PCR, we observed no significant difference in expression of RNA in the brains of both models compared with WT mice (Fig. 2, *A* and *B*, and data not shown), which is in agreement with the original reports on these models (26, 27). Our N-terminal anti-Pam antibody PF3 detected a stable truncated Pam protein in homozygous $Phr1^{Mag}$ mice brain lysates (Fig. 2*A*, *right panel*), which is consistent with the earlier study (26). However, PF3 was unable to detect a stable protein product in homozygous $Phr1^{\Delta 8,9}$ mouse brain lysates with an in-frame deletion of exons 8 and 9 (Fig. 2*B*, *middle panel*), which could be due to masking of the epitope of the antibody employed. Using anti-MYCBP2 antibody (ab86078, Abcam), which was raised against Pam amino acids 2425–2475, we observed expression of Phr1 at a significantly reduced level in $Phr1^{\Delta 8,9}$ mutant mouse brain compared with WT littermate brain (Fig. 2*B*, *right panel*). Protein expression of Phr1 in the $Phr1^{\Delta 8,9}$ model has not been reported earlier. Given these observations, we cannot rule out the possibility that this extremely large protein is unstable under our experimental conditions.

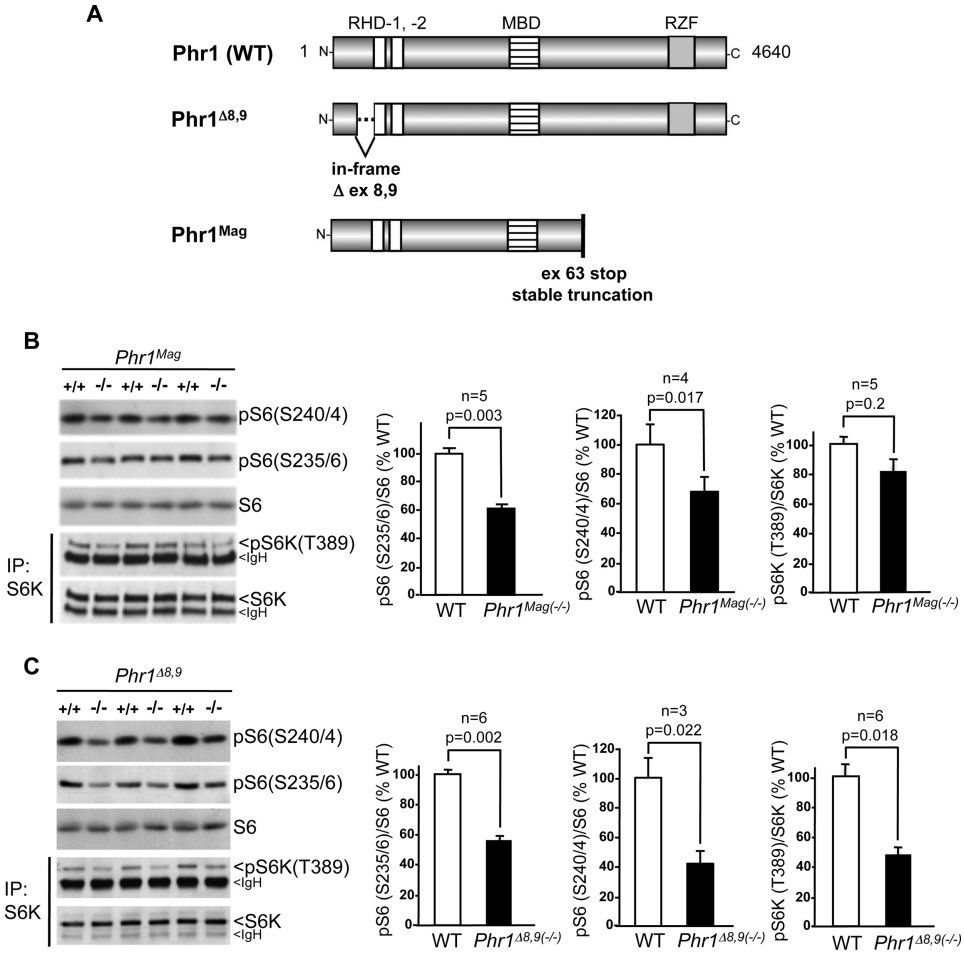

FIGURE 1. **Compromised mTORC1 signaling in two different *Phr1* mutant mouse models.** *A*, schematic of WT and mutant Phr1 protein products. WT Phr1 includes RHD-1 and RHD-2, a Myc-binding domain (*MBD*), and an RZF domain. The $Phr1^{\Delta 8,9}$ allele has an in-frame deletion of exons (*ex*) 8 and 9, and the $Phr1^{Mag}$ allele has a stop codon at exon 63 encoding a stable truncation protein product. *B* and *C*, *left panels*, immunoblotting demonstrated reduced levels of phospho-S6 (*pS6*) and phospho-S6K (*pS6K*) in E17.5–18.5 brains from homozygous $Phr1^{Mag}$ (−/−; *B*) and $Phr1^{\Delta 8,9}$ (−/−; *C*) mutant mice compared with the respective WT littermates (+/+). Immunoprecipitation (*IP*) was performed using anti-S6K antibody. *Right panels*, quantitative and statistical analyses of WT and mutant animal pairs are shown for phospho-S6 (Ser-235/Ser-236 and Ser-240/Ser-244) and phospho-S6K (Thr-389), relative to total S6 and S6K levels, respectively. *IgH*, immunoglobulin heavy chain. Experiments were carried out with two independent litters.

Increased Levels of TSC1/2 in $Phr1^{Mag}$ Mouse Brain but Not in $Phr1^{\Delta 8,9}$ Mouse Brain—We showed previously that Pam binds to the TSC1-TSC2 complex and that the RZF motif in Pam is responsible for ubiquitinating TSC2 (7, 23). Based on these results, in the absence of the Ub ligase activity, the TSC2 protein level is expected to increase in $Phr1^{Mag}$ mouse brain lacking the RZF motif (Ub ligase domain). We therefore examined the protein levels of TSC1 and TSC2 in brain lysates of $Phr1^{Mag}$ and $Phr1^{\Delta 8,9}$ mice. Both the TSC1 and TSC2 protein levels were increased in $Phr1^{Mag}$ mutants compared with the wild-type littermate controls; however, the levels of TSC1 and TSC2 proteins did not change in $Phr1^{\Delta 8,9}$ mutants compared with the respective control littermates (Fig. 3). Quantitative RT-PCR analysis of *Tsc1* and *Tsc2* revealed no change in the RNA levels in $Phr1^{Mag}$ mutants (data not shown), consistent with Pam acting as an E3 Ub ligase to regulate stability of TSC proteins. Our results also suggest that the down-regulation of mTORC1 observed in $Phr1^{\Delta 8,9}$ mice is not mediated through the TSC proteins. Genetic studies have established the dual-leucine zipper kinase DLK1/Wallenda as the E3 Ub ligase target in both *C. elegans* (RPM-1) and *Drosophila* (HIW) (16–18). However, we did not observe any change in the levels of mammalian DLK in either $Phr1^{Mag}$ or $Phr1^{\Delta 8,9}$ mutant mice (Fig. 3), consistent with other studies reporting that DLK or p38 MAPK signaling is not involved in either mouse (*Phr1*) or zebrafish (*esrom*) mutant phenotypes (27, 31).

Exogenous Expression of Either N- or C-terminal Segments of Pam Activates mTORC1 Signaling—Our data document that either in-frame disruption of two exons at the N terminus or deletion of the C terminus of *Phr1* is associated with down-regulation of mTORC1 signaling. We therefore tested the possibility that overexpression of N- and C-terminal segments of Pam will result in activation of mTORC1 signaling. To determine whether Pam overexpression could constitutively activate mTORC1 signaling, Myc-tagged Pam N-terminal segment F1 (Myc-PamF1) containing the RHD (amino acids 1–1669) or Myc-tagged Pam C-terminal segment F3 (Myc-PamF3) with the RZF domain (amino acids 3448–4640) (Fig. 4*A*) was coexpressed with the HA-S6K reporter in HEK293T cells, serum-deprived overnight, and examined for S6K activation. Both the N- and C-terminal segments of Pam activated S6K phosphorylation in a dose-dependent manner as detected by phosphory-

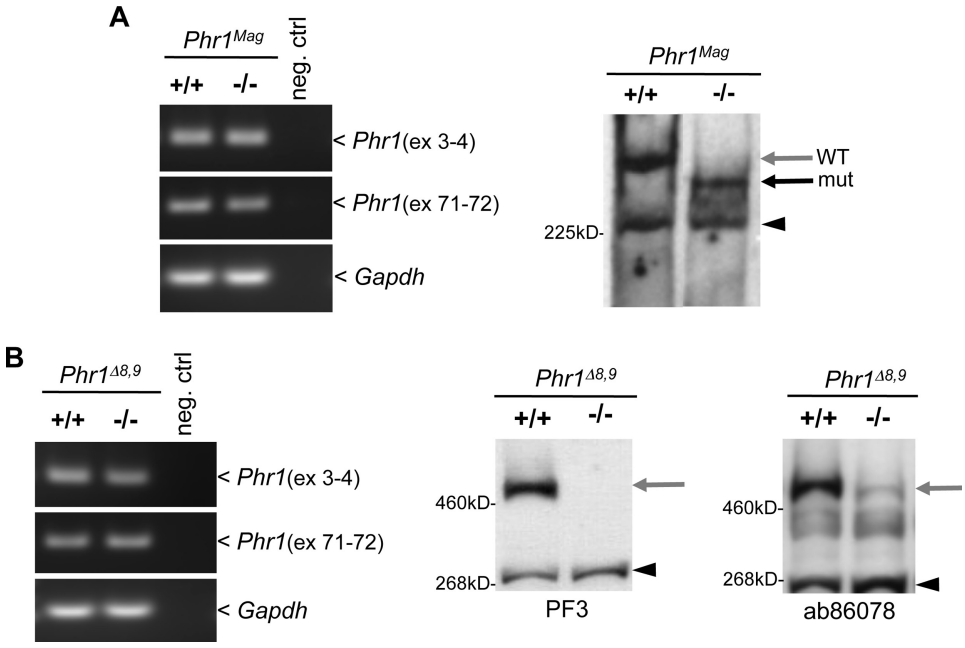

FIGURE 2. **Expression of Phr1 in embryonic brains from *Phr1* mouse models.** *A*, *left panel*, RT-PCR of E17.5 brain cDNA from $Phr1^{Mag}$ mutant (−/−) and WT (+/+) littermates showed stable *Phr1* transcript expression. *Right panel*, utilizing the anti-Phr1 polyclonal antibody PF3, immunoblotting of E17.5 brain from the $Phr1^{Mag}$ mouse model demonstrated expression of the WT (*gray arrow*) and the C-terminally truncated protein product (*mut*; *black arrow*) in homozygous mutant (−/−) *versus* WT (+/+) littermates. *neg. ctrl*, negative control; *ex*, exons. *B*, *left panel*, RT-PCR of $Phr1^{\Delta 8,9}$ mutant brain cDNA also showed stable *Phr1* transcript expression in mutant (−/−) compared with WT (+/+) littermates. Immunoblotting of E17.5 brain lysates from the $Phr1^{\Delta 8,9}$ model showed that the N-terminal polyclonal antibody PF3 was unable to detect the Phr1 mutant protein possessing an in-frame N-terminal deletion (*middle panel*), whereas anti-MYCBP2 antibody (ab86078) detected Phr1 (*gray arrows*) at a reduced level in mutant (−/−) mouse brain compared with a WT (+/+) littermate (*right panel*). GAPDH served as a control for RT-PCR. *Arrowheads* indicate nonspecific bands.

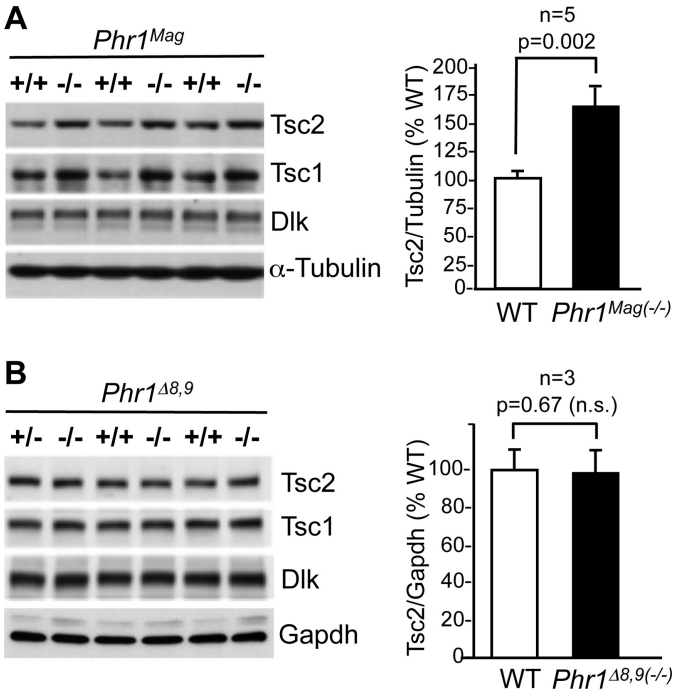

FIGURE 3. **Increased levels of TSC1/2 in embryonic brains of $Phr1^{Mag}$ mice, but not in $Phr1^{\Delta 8,9}$ mice.** *A*, *left panel*, immunoblotting of E17.5–18.5 brain lysates from $Phr1^{Mag}$ mice showed increased levels of TSC1/2 in homozygous mutant (−/−) mice compared with WT (+/+) littermates with no change in DLK levels. *B*, *left panel*, immunoblotting of E17.5–18.5 brain lysates from $Phr1^{\Delta 8,9}$ mice showed comparable levels of both TSC1/2 and DLK in WT (+/+) and homozygous mutant (−/−) littermates. *Right panels*, quantitative analyses of WT and mutant animal pairs are shown. *n.s.*, not significant. The intensities of TSC2 and DLK were normalized to α-tubulin or GAPDH. Experiments were carried out with two independent litters.

lation of S6K at Thr-389 (Fig. 4, *B* and *C*). Based on the ability of Pam to increase [^{35}S]GTPγS binding to Rheb as well as the release of tritiated [^{3}H]-GDP from Rheb, it was suggested that Pam may act as a GEF for Rheb through its RHD (32). We asked whether Rheb is required for the ability of the PamF1 fragment containing the RHD to activate mTORC1 by employing RNAi-mediated knockdown of Rheb, followed by exogenous expression of PamF1 in HEK293T cells. The activation of S6K by PamF1 under serum-deprived conditions was partially blocked by Rheb RNAi, suggesting that Rheb may be partly responsible for the activation of S6K by PamF1 (Fig. 4*D*). A decrease in S6K activation by Rheb RNAi in insulin-stimulated cells served as a positive functional readout for Rheb RNAi in these cells (Fig. 4*E*). As expected, activation of S6K by PamF1 and PamF3 was blocked by rapamycin as well as by amino acid deprivation (data not shown).

Functional Complementation between $Phr1^{Mag}$ and $Phr1^{\Delta 8,9}$ Mice with Respect to mTORC1 Signaling—To further validate that Pam regulates mTORC1 signaling *in vivo* through two functionally independent domains, we generated a compound heterozygous model by crossing heterozygous $Phr1^{Mag}$ mice ($Phr1^{Mag/+}$) with heterozygous $Phr1^{\Delta 8,9}$ mice ($Phr1^{\Delta 8,9/+}$) (Fig. 5*A*). The compound heterozygous $Phr1^{\Delta 8,9/Mag}$ mutants, similar to the homozygous $Phr1^{Mag}$ and $Phr1^{\Delta 8,9}$ mutants, displayed neonatal lethality, indicating that one WT copy of *Phr1* is required for survival. However, mTORC1 signaling (as reflected by phosphorylation of S6K at Thr-389 and of S6 at Ser-240/Ser-244) was not compromised in brain samples obtained from at least 11 compound heterozygous mice compared with either WT or heterozygous littermates. Genotyping

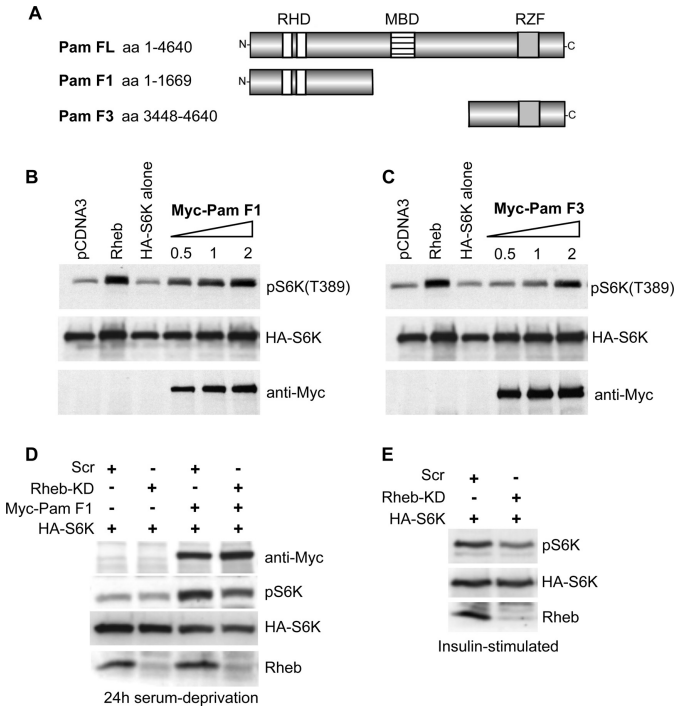

FIGURE 4. **Overexpression of either N- or C-terminal fragments of Pam induces S6K phosphorylation in a dose-dependent manner.** *A*, schematic of full-length (*FL*) Pam, the N-terminal fragment (amino acids (*aa*) 1–1669) containing RHD-1 and RHD-2 (PamF1), and the C-terminal fragment (amino acids 3448–4640) containing the RZF domain of Pam (PamF3). *MBD*, Myc-binding domain. *B* and *C*, overexpression of the indicated amounts (micrograms) of Myc-PamF1 (*B*) and Myc-PamF3 (*C*) along with an HA-S6K reporter in HEK293T cells resulted in an increased level of phospho-S6K (*pS6K*) compared with controls (pcDNA3 vector, HA-S6K alone) under serum-deprived conditions. Overexpression of Rheb served as a positive control. *D*, in serum-deprived HEK293T cells overexpressing Myc-PamF1 along with an HA-S6K reporter (*third* and *fourth lanes*), transduction of Rheb shRNA (Rheb-*KD*) resulted in inhibition of phospho-S6K (*fourth lane*) compared with scrambled (*Scr*) control shRNA (*third lane*). The *first* and *second lanes* served as controls. *E*, as expected, transduction of Rheb shRNA in HEK293T cells resulted in decreased S6K phosphorylation upon insulin stimulation compared with scrambled control shRNA. Immunoblotting using anti-Myc and anti-HA antibodies served as a control. The results are representative of three independent experiments.

and immunoblotting data from a representative $Phr1^{\Delta 8,9/Mag}$ litter are shown in Fig. 5 (*B* and *C*). These results indicate that mTORC1 down-regulation is not responsible for lethality at birth. Importantly, in $Phr1^{\Delta 8,9/Mag}$mice, an intact N terminus on the $Phr1^{Mag}$ allele and an intact C terminus on the $Phr1^{\Delta 8,9}$ allele displayed functional complementation with respect to mTORC1 signaling, but not neonatal lethality. Taken together, our results suggest that the N terminus (putative GEF) and the C terminus (Ub ligase) of Pam independently regulate mTORC1 signaling *in vivo*. Homozygous $Phr1^{\Delta 8,9}$ mutant mice exhibit CNS morphology defects, including corpus callosum defects, loss of internal capsule axon fiber tracts, and loss of the anterior commissure, among many other observed defects (27). The CNS morphology defects have not been described previously for homozygous $Phr1^{Mag}$ mice (26); therefore, we examined E18.5 brain sections of these mutant mice by histology and observed a number of defects, including loss of internal capsule axon fiber tracts, absence of anterior commissure, and a narrower corpus callosum (Fig. 6, *A* and *B*, and data not shown). We then raised the question of whether any of these defects could be rescued in the compound heterozygous $Phr1^{\Delta 8,9/Mag}$ mice, in which mTORC1 signaling is not compromised. Interestingly, we observed that the thinner corpus callosum seen in homozygous $Phr1^{\Delta 8,9}$ and $Phr1^{Mag}$ mice was consistently rescued in eight of eight (four litters) compound heterozygous $Phr1^{\Delta 8,9/Mag}$ mice and was indistinguishable from the WT littermates (Fig. 6, *C–E*). However, the defects in axon fiber tracts of the internal capsule and anterior commissure persisted in the compound heterozygous mice (Fig. 6, *F–H* ; and data not shown), strongly suggesting that these defects are mTORC1-independent.

Fbxo45 May Not Play a Role in the Regulation of mTORC1 Signaling by Pam—FSN-1 family F-box proteins are physical and functional partners for Pam and its homologs (18, 33, 34). F-box proteins generally are target recognition modules for SCF (Skp/cullin/F-box) E3 Ub ligase complexes (35). The *C. elegans fsn-1* and *Drosophila DFsn* mutants exhibit synaptic defects that phenocopy *rpm-1* and *hiw* mutants, respectively (18, 33). The FSN-1 vertebrate homolog Fbxo45, which is restricted to the nervous system, forms an E3 Ub ligase complex that includes Skp1; however, instead of interacting through cullin, Fbxo45 and Pam interact directly through the SPRY domain and Myc-binding domain, respectively, diverging from traditional SCF E3 ligase complexes (34). Although homozygous *Fbxo45* knock-out mice exhibit many phenotypes resembling $Phr1^{Mag}$ and $Phr1^{\Delta 8,9}$ mutant mice, they do not show defects in the corpus callosum (34). We raised the question of whether Fbxo45 levels are altered in *Phr1* mutants and observed a reduction at the protein level in both $Phr1^{Mag}$ and $Phr1^{\Delta 8,9}$ mutant brain lysates with no change at the RNA level (Fig. 7, *A* and *B*). Fbxo45 was also reduced in compound heterozygous $Phr1^{\Delta 8,9/Mag}$ mutant mice (Fig. 7*C*), suggesting that at least one intact wild-type copy of Pam is required for Fbxo45 stability. In addition, unlike Pam, overexpressed Fbxo45 was unable to activate mTORC1 signaling (Fig. 7*D*). Taken together, these data suggest that Pam regulates mTORC1 independently of Fbxo45.

DISCUSSION

Pam is a large multidomain protein with a putative GEF homology domain at the N terminus, a Myc-interacting domain in the middle, and a C-terminal RZF domain typical of E3 Ub ligases (9, 10). Our earlier studies showed that the C-terminal domain of Pam interacts with the TSC1-TSC2 complex and regulates mTORC1 signaling by ubiquitinating TSC2 (7, 23). In this study, we have demonstrated that both the N- and C-terminal domains of Pam independently regulate mTORC1 signaling *in vitro* and *in vivo*. Two independent mutant mouse models of Pam, $Phr1^{\Delta 8,9}$ with an intact C terminus and $Phr1^{Mag}$ with a deletion of the C-terminal RZF domain but a stably expressed N-terminal domain, show down-regulation of mTORC1 as observed by decreased phosphorylation of downstream targets S6K and S6. However, phosphorylation of another mTOR target, 4E-BP1, was not affected, consistent with other studies in which differential regulation of mTORC1 downstream targets was reported (36, 37). In agreement with the loss of either the N or C terminus of Pam resulting in down-regulation of mTORC1, overexpression of either the N or C terminus of Pam activates mTORC1 signaling.

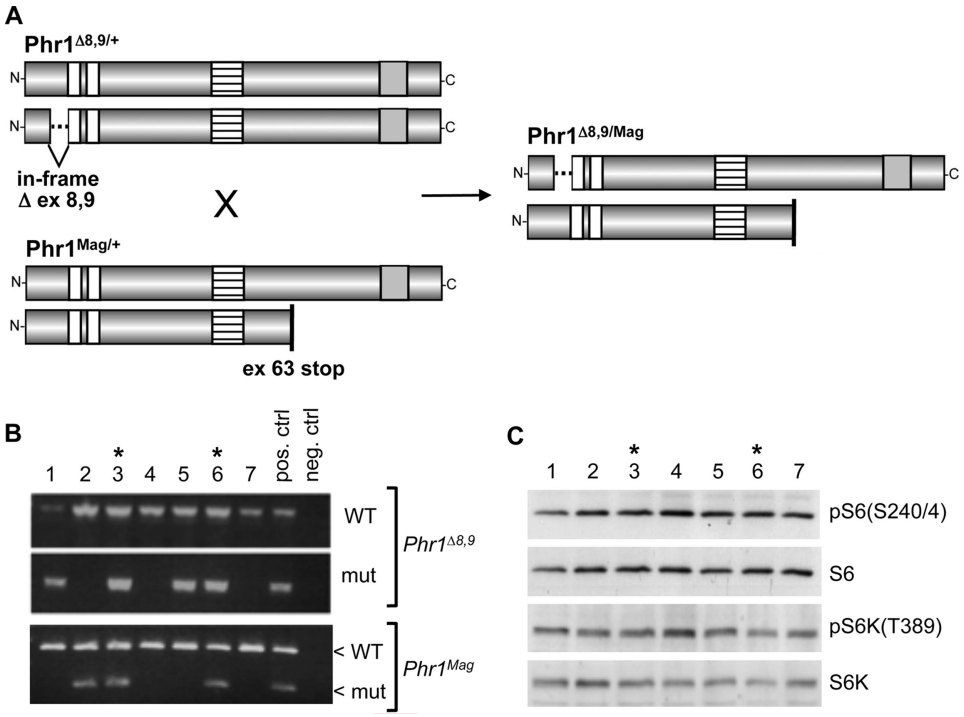

FIGURE 5. **N- and C-terminal Pam regions display functional complementation of mTORC1 signaling in a compound heterozygous mouse model.** *A*, mating scheme for generating a compound heterozygous model (*Phr1*$^{\Delta 8,9/Mag}$) by crossing heterozygous *Phr1*$^{Mag/+}$ and heterozygous *Phr1*$^{\Delta 8,9/+}$ mice. *ex*, exon. *B*, genomic PCR genotyping of a representative litter demonstrates WT (*lanes 4* and *7*), heterozygous *Phr1*$^{\Delta 8,9/+}$ (*lanes 1* and *5*), and heterozygous *Phr1*$^{Mag/+}$ (*lane 2*) mice. *Asterisks* indicate compound heterozygous *Phr1*$^{\Delta 8,9/Mag}$ mice (*lanes 3* and *6*). *pos. ctrl* and *neg. ctrl*, positive and negative controls, respectively; *mut*, mutant. *C*, immunoblotting of E17.5 brain lysates from a representative mouse litter (lane assignments as in (B)) demonstrated comparable phospho-S6 (*pS6*) and phospho-S6K (*pS6K*) levels in compound heterozygous *Phr1*$^{\Delta 8,9/Mag}$ mice (*lanes 3* and *6*) compared with WT or single heterozygous littermates. *Asterisks* indicate compound heterozygous *Phr1*$^{\Delta 8,9/Mag}$ mice. S6 and S6K served as controls. mTOR signaling was examined in brain lysates from 11 compound heterozygous mice.

RHDs have been shown to function as GEFs and stimulate the nucleotide release of small GTPases such as Arf, Rab, and Ran (38). It was recently demonstrated that sphingosine 1-phosphate-induced activation of mTORC1 is mediated by Pam and that Pam may act as a GEF for Rheb (32). Our results show that Rheb may be partly responsible for activation of mTORC1 mediated by the N terminus of Pam; however, it cannot be ruled out that other yet to be defined mechanisms could also play a role in this regulation. Further studies are necessary to understand whether Pam binds to Rheb directly or indirectly as well as whether Pam acts as a *bona fide* Rheb GEF *in vivo*. The large size of the Pam protein (~500 kDa) and the inherent difficulties in reliably assaying Rheb GDP/GTP ratios make these studies quite challenging.

It is interesting that the down-regulation of mTORC1 signaling is restricted to brain in *Phr1* mouse models, which may be explained by dosage-sensitive effects of Pam loss in the brain. Alternatively, we raised the possibility that HERC1, a 532-kDa E3 Ub ligase with striking structural similarity to Pam and identified as a TSC2 interactor (39), plays a similar role as Pam and compensates for the loss of Pam in tissues other than brain. Interestingly, HERC1 has a C-terminal HECT domain, a hallmark of E3 Ub ligases, as well as an RHD at the N terminus and has been shown to ubiquitinate TSC2 *in vitro* (39). Therefore, it is tempting to speculate that, similar to Pam, HERC1 could exhibit two distinct modes of regulation on TSC/mTORC1 signaling and that these two large structurally similar proteins could function in a tissue/context-specific manner.

Our observation that the down-regulation of mTORC1 seen in both homozygous *Phr1* mutants is rescued in compound heterozygous *Phr1*$^{\Delta 8,9/Mag}$ mice clearly documents that the N and C termini of Pam can functionally complement each other with respect to mTORC1 regulation. However, similar to the homozygous *Phr1*$^{\Delta 8,9}$ and *Phr1*^{Mag} mutant mice, the compound heterozygous mutants die at birth, suggesting that mTORC1 down-regulation is not responsible for perinatal lethality and at least one intact wild-type *Phr1* allele is required for survival. In addition to defects in sensory and motor neurons, *Phr1* knock-out mice exhibit a severe reduction of major axon tracts in the CNS, with narrowing and reduced thickness of the corpus callosum and absence of the anterior commissure (27). We have shown that the narrower corpus callosum seen in homozygous *Phr1*$^{\Delta 8,9}$ and *Phr1*^{Mag} mutant mice is rescued in compound heterozygous *Phr1*$^{\Delta 8,9/Mag}$ mice, supporting the notion that down-regulation of mTORC1 signaling may be responsible for the corpus callosum defects in *Phr1* mutant mice. However, other CNS defects persist in the double heterozygous mice, suggesting that they are not mTORC1-dependent. Our results also imply that Pam may regulate mTORC1 signaling independently of Fbxo45, which is consistent with a previous report showing no change in TSC2 protein levels in Fbxo45-deficient mouse brain (34). It is interesting that although Fbxo45 knock-out mice resemble *Phr1*$^{\Delta 8,9}$ mice, with a loss of major axon tracts and the complete absence of the anterior commissure, they differ from *Phr1*$^{\Delta 8,9}$ mice in that

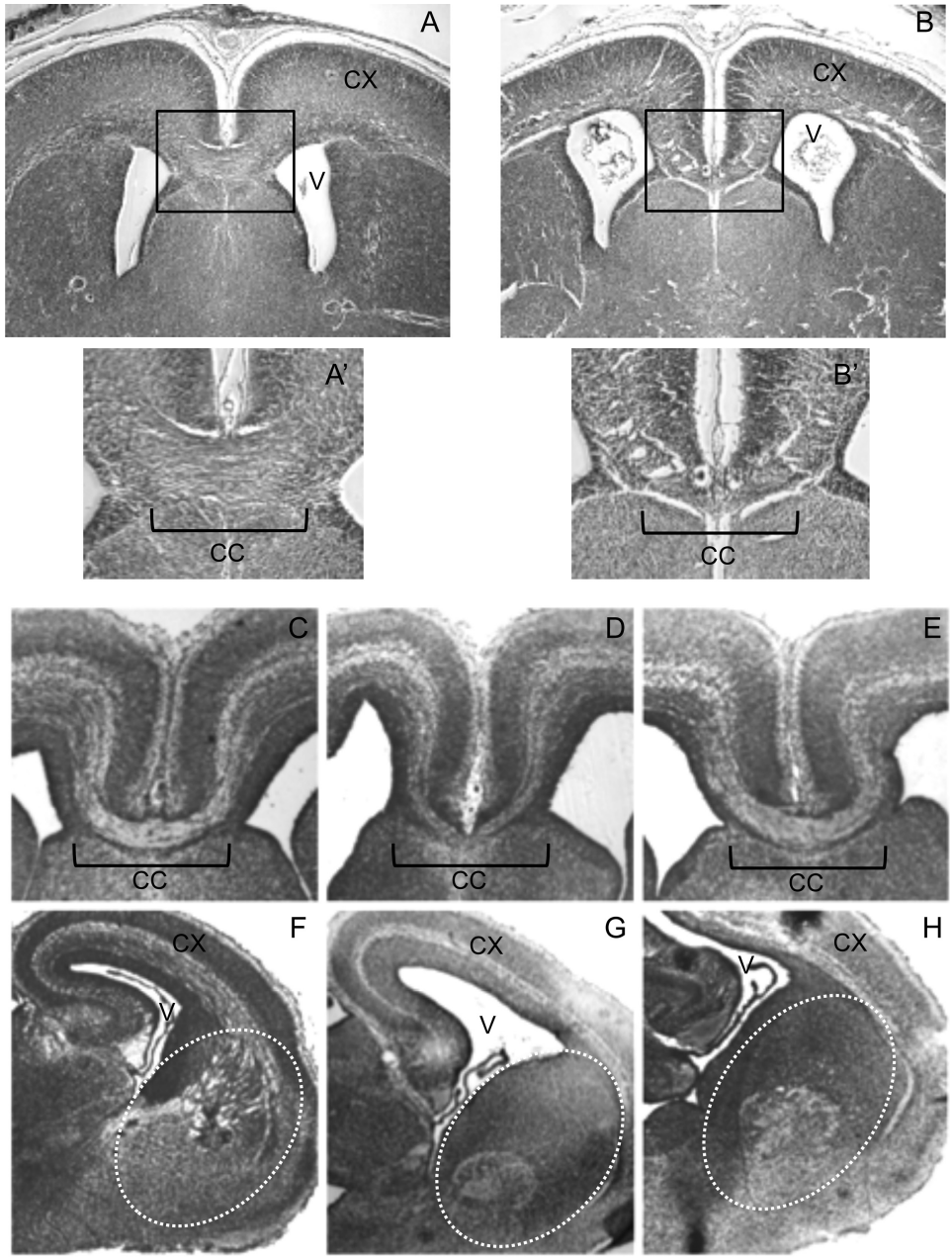

FIGURE 6. **Structural defects in the brains of *Phr1* mutant mouse models.** *A* and *B*, representative hematoxylin and eosin staining of paraffin-embedded E18.5 coronal brain sections (6-μm step sections) from $Phr1^{+/+}$ (*A* and *A′*) and $Phr1^{Mag/Mag}$ (*B* and *B′*) mice is shown. A structural defect in the anterior region of the corpus callosum (*CC*, *bracketed region*) was observed in homozygous $Phr1^{Mag}$ mice (*B*) compared with $Phr1^{+/+}$ littermates (*A*). *Boxed regions* in *A* and *B* are enlarged in *A′* and *B*, respectively. *C–H*, representative images of cresyl violet-stained coronal cyrosections (20-μm thickness) from E18.5 $Phr1^{+/+}$ (*C* and *F*), $Phr1^{\Delta 8,9/\Delta 8,9}$ (*D* and *G*), and compound heterozygous $Phr1^{\Delta 8,9/Mag}$ (*E* and *H*) mouse brains are shown. *C–E*, the rescued phenotype of the corpus callosum in compound heterozygous mice is shown. Rescue of the corpus callosum was seen in eight of eight compound heterozygous mice examined. Note the indistinguishable corpus callosum morphology of WT (*C*) and compound heterozygous $Phr1^{\Delta 8,9/Mag}$ (*E*) mice in contrast to the thinning of the corpus callosum in $Phr1^{\Delta 8,9/\Delta 8,9}$ mice (*D*). *F–H*, similar to $Phr1^{\Delta 8,9/\Delta 8,9}$ mice (*G*), developing axons in the internal capsule (*dashed oval regions*) are bundled into a single large fascicle and are displaced ventromedially in compound heterozygous $Phr1^{\Delta 8,9/Mag}$ mice (*H*) compared with wild-type littermates (*F*). *CX*, cortex; *V*, lateral ventricle.

they have no defect in the corpus callosum (34). It is likely that the Pam-Fbxo45 Ub ligase complex could target other proteins/pathways, which, when dysregulated, might result in neural development defects shared between the $Phr1^{\Delta 8,9}$- and *Fbxo45*-deficient mice.

mTORC1-mediated signaling plays an important role in neurodevelopment by modulating both general and neuronal activity-dependent protein synthesis. More importantly, long-lasting forms of synaptic plasticity and memory are dependent on new protein synthesis, and aberrant mTORC1 signaling is reported in many neurological disorders and has emerged as a common biochemical characteristic of many syndromes associated with autism spectrum disorders (6, 40, 41). Recent evidence indicates that mutations in genes such as *NLGN3/4*, *SHANK3*, and *NRXN1* are associated with altered synaptic function and lead to autism/Asperger syndrome, and the

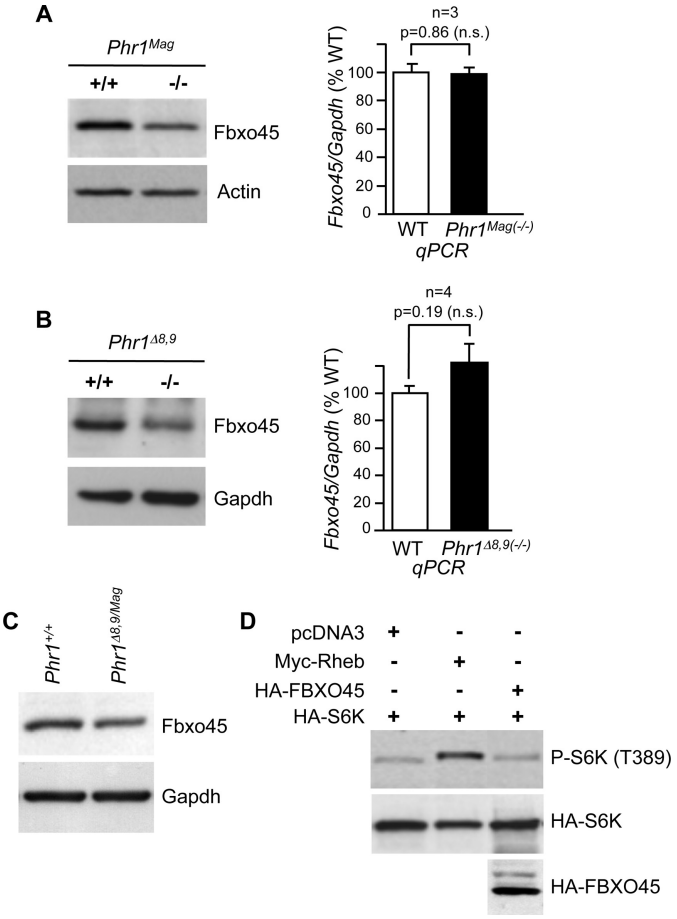

FIGURE 7. **Reduced Fbxo45 levels in both *Phr1* mutant mouse models.** *A* and *B*, whole brain lysates and RNA were prepared from E17.5–18.5 littermates and subjected to Western blot and real-time quantitative PCR (*qPCR*) analyses. Immunoblotting of at least three WT and mutant animal pairs showed diminished levels of Fbxo45 in both $Phr1^{Mag}$ (−/−) (*A*) and $Phr1^{\Delta 8,9}$ (−/−) mice (*B*) compared with the respective WT (+/+) mice. Representative immunoblots are shown (*left panels*). Actin and GAPDH served as loading controls. For quantitative PCR analyses of both Phr1 mouse models, expression of *Fbxo45* mRNA in embryonic mouse brains from at least three WT and mutant animal pairs is shown (*right panels*). GAPDH was used for normalization. *n.s.*, not significant. *C*, immunoblotting of compound heterozygous $Phr1^{\Delta 8,9/Mag}$ mouse brain also demonstrated a decreased level of Fbxo45 compared with WT (+/+) littermates. Experiments represented in *A–C* were carried out with two independent litters. *D*, overexpression of HA-Fbxo45 along with an HA-S6K reporter in HEK293T cells did not result in increased phosphorylation of S6K under serum-deprived conditions. Myc-Rheb and the pcDNA3 vector alone served as positive and negative controls, respectively.

NLGN/SHANK3/NRXN pathway is also linked to synaptogenesis (4, 42). Pam and its homologs function as regulators of synapse formation and growth, and work from our laboratory has shown Pam to be a TSC/mTORC1 pathway regulator in neurons. Therefore, it is tempting to speculate whether an interplay between synaptic protein synthesis and degradation could be critical in axon branching and synaptogenesis and whether Pam acts as a key player in regulating synaptic protein synthesis through mTORC1 signaling and synaptic protein degradation as an E3 Ub ligase. Identifying key neuronal targets of Pam will have direct relevance for diverse aspects of neural development and neural connectivity, as regulated protein degradation by the Ub-proteasome system is essential for synaptic connections.

Acknowledgments—We thank Drs. Samuel L. Pfaff and Joseph Lewcock for generously providing the $Phr1^{Mag}$ mutant mice and Drs. Lawrence Holzman and Hideyuki Okano for providing antibodies to DLK and Fbxo45, respectively.

REFERENCES

1. Crino, P. B., Nathanson, K. L., and Henske, E. P. (2006) The tuberous sclerosis complex. *N. w Engl. J. Med.* **355,** 1345–1356
2. Han, J. M., and Sahin, M. (2011) TSC1/TSC2 signaling in the CNS. *FEBS Lett.* **585,** 973–980
3. Huang, J., and Manning, B. D. (2008) The TSC1-TSC2 complex: a molecular switchboard controlling cell growth. *Biochem. J.* **412,** 179–190
4. Bourgeron, T. (2009) A synaptic trek to autism. *Curr. Opin. Neurobiol.* **19,** 231–234
5. Dazert, E., and Hall, M. N. (2011) mTOR signaling in disease. *Curr. Opin. Cell Biol.* **23,** 744–755
6. Kelleher, R. J., 3rd, and Bear, M. F. (2008) The autistic neuron: troubled translation? *Cell* **135,** 401–406
7. Murthy, V., Han, S., Beauchamp, R. L., Smith, N., Haddad, L. A., Ito, N., and Ramesh, V. (2004) Pam and its ortholog Highwire interact with and may negatively regulate the TSC1-TSC2 complex. *J. Biol. Chem.* **279,** 1351–1358
8. Joazeiro, C. A., and Weissman, A. M. (2000) RING finger proteins: mediators of ubiquitin ligase activity. *Cell* **102,** 549–552
9. Guo, Q., Xie, J., Dang, C. V., Liu, E. T., and Bishop, J. M. (1998) Identification of a large Myc-binding protein that contains RCC1-like repeats. *Proc. Natl. Acad. Sci. U.S.A.* **95,** 9172–9177
10. Po, M. D., Hwang, C., and Zhen, M. (2010) PHRs: bridging axon guidance, outgrowth, and synapse development. *Curr. Opin. Neurobiol.* **20,** 100–107
11. Burgess, R. W., Peterson, K. A., Johnson, M. J., Roix, J. J., Welsh, I. C., and O'Brien, T. P. (2004) Evidence for a conserved function in synapse formation reveals *Phr1* as a candidate gene for respiratory failure in newborn mice. *Mol. Cell. Biol.* **24,** 1096–1105
12. D'Souza, J., Hendricks, M., Le Guyader, S., Subburaju, S., Grunewald, B., Scholich, K., and Jesuthasan, S. (2005) Formation of the retinotectal projection requires Esrom, an ortholog of Pam (protein associated with Myc). *Development* **132,** 247–256
13. Schaefer, A. M., Hadwiger, G. D., and Nonet, M. L. (2000) *rpm-1*, a conserved neuronal gene that regulates targeting and synaptogenesis in *C. elegans*. *Neuron* **26,** 345–356
14. Wan, H. I., DiAntonio, A., Fetter, R. D., Bergstrom, K., Strauss, R., and Goodman, C. S. (2000) Highwire regulates synaptic growth in *Drosophila*. *Neuron* **26,** 313–329
15. Zhen, M., Huang, X., Bamber, B., and Jin, Y. (2000) Regulation of presynaptic terminal organization by *C. elegans* RPM-1, a putative guanine nucleotide exchanger with a RING-H2 finger domain. *Neuron* **26,** 331–343
16. Collins, C. A., Wairkar, Y. P., Johnson, S. L., and DiAntonio, A. (2006) Highwire restrains synaptic growth by attenuating a MAP kinase signal. *Neuron* **51,** 57–69
17. Nakata, K., Abrams, B., Grill, B., Goncharov, A., Huang, X., Chisholm, A. D., and Jin, Y. (2005) Regulation of a DLK-1 and p38 MAP kinase pathway by the ubiquitin ligase RPM-1 is required for presynaptic development. *Cell* **120,** 407–420
18. Wu, C., Daniels, R. W., and DiAntonio, A. (2007) DFsn collaborates with Highwire to down-regulate the Wallenda/DLK kinase and restrain synaptic terminal growth. *Neural Dev.* **2,** 16
19. McCabe, B. D., Hom, S., Aberle, H., Fetter, R. D., Marques, G., Haerry, T. E., Wan, H., O'Connor, M. B., Goodman, C. S., and Haghighi, A. P. (2004) Highwire regulates presynaptic BMP signaling essential for synaptic growth. *Neuron* **41,** 891–905
20. Pierre, S. C., Häusler, J., Birod, K., Geisslinger, G., and Scholich, K. (2004) Pam mediates sustained inhibition of cAMP signaling by sphingosine 1-phosphate. *EMBO J.* **23,** 3031–3040
21. Grill, B., Bienvenut, W. V., Brown, H. M., Ackley, B. D., Quadroni, M., and Jin, Y. (2007) *C. elegans* RPM-1 regulates axon termination and synapto-

genesis through the Rab GEF GLO-4 and the Rab GTPase GLO-1. *Neuron* **55,** 587–601
22. Wu, C., Wairkar, Y. P., Collins, C. A., and DiAntonio, A. (2005) Highwire function at the *Drosophila* neuromuscular junction: spatial, structural, and temporal requirements. *J. Neurosci.* **25,** 9557–9566
23. Han, S., Witt, R. M., Santos, T. M., Polizzano, C., Sabatini, B. L., and Ramesh, V. (2008) Pam (protein associated with Myc) functions as an E3 ubiquitin ligase and regulates TSC/mTOR signaling. *Cell. Signal.* **20,** 1084–1091
24. DiAntonio, A., and Hicke, L. (2004) Ubiquitin-dependent regulation of the synapse. *Annu. Rev. Neurosci.* **27,** 223–246
25. Kawabe, H., and Brose, N. (2011) The role of ubiquitylation in nerve cell development. *Nat. Rev. Neurosci.* **12,** 251–268
26. Lewcock, J. W., Genoud, N., Lettieri, K., and Pfaff, S. L. (2007) The ubiquitin ligase Phr1 regulates axon outgrowth through modulation of microtubule dynamics. *Neuron* **56,** 604–620
27. Bloom, A. J., Miller, B. R., Sanes, J. R., and DiAntonio, A. (2007) The requirement for *Phr1* in CNS axon tract formation reveals the corticostriatal boundary as a choice point for cortical axons. *Genes Dev.* **21,** 2593–2606
28. Han, S., Santos, T. M., Puga, A., Roy, J., Thiele, E. A., McCollin, M., Stemmer-Rachamimov, A., and Ramesh, V. (2004) Phosphorylation of tuberin as a novel mechanism for somatic inactivation of the tuberous sclerosis complex proteins in brain lesions. *Cancer Res.* **64,** 812–816
29. Santos, T. M., Han, S., Bowser, M., Sazani, K., Beauchamp, R. L., Murthy, V., Bhide, P. G., and Ramesh, V. (2006) Alternative splicing in protein associated with Myc (Pam) influences its binding to c-Myc. *J. Neurosci. Res.* **83,** 222–232
30. James, M. F., Han, S., Polizzano, C., Plotkin, S. R., Manning, B. D., Stemmer-Rachamimov, A. O., Gusella, J. F., and Ramesh, V. (2009) NF2/merlin is a novel negative regulator of mTOR complex 1, and activation of mTORC1 is associated with meningioma and schwannoma growth. *Mol. Cell. Biol.* **29,** 4250–4261
31. Hendricks, M., and Jesuthasan, S. (2009) PHR regulates growth cone pausing at intermediate targets through microtubule disassembly. *J. Neurosci.* **29,** 6593–6598
32. Maeurer, C., Holland, S., Pierre, S., Potstada, W., and Scholich, K. (2009) Sphingosine 1-phosphate-induced mTOR activation is mediated by the E3 ubiquitin ligase Pam. *Cell. Signal.* **21,** 293–300
33. Liao, E. H., Hung, W., Abrams, B., and Zhen, M. (2004) An SCF-like ubiquitin ligase complex that controls presynaptic differentiation. *Nature* **430,** 345–350
34. Saiga, T., Fukuda, T., Matsumoto, M., Tada, H., Okano, H. J., Okano, H., and Nakayama, K. I. (2009) Fbxo45 forms a novel ubiquitin ligase complex and is required for neuronal development. *Mol. Cell. Biol.* **29,** 3529–3543
35. Deshaies, R. J. (1999) SCF and cullin/RING H2-based ubiquitin ligases. *Annu. Rev. Cell Dev. Biol.* **15,** 435–467
36. Choo, A. Y., Yoon, S. O., Kim, S. G., Roux, P. P., and Blenis, J. (2008) Rapamycin differentially inhibits S6Ks and 4E-BP1 to mediate cell type-specific repression of mRNA translation. *Proc. Natl. Acad. Sci. U.S.A.* **105,** 17414–17419
37. Hoeffer, C. A., Tang, W., Wong, H., Santillan, A., Patterson, R. J., Martinez, L. A., Tejada-Simon, M. V., Paylor, R., Hamilton, S. L., and Klann, E. (2008) Removal of FKBP12 enhances mTOR-Raptor interactions, LTP, memory, and perseverative/repetitive behavior. *Neuron* **60,** 832–845
38. Rosa, J. L., Casaroli-Marano, R. P., Buckler, A. J., Vilaró, S., and Barbacid, M. (1996) p619, a giant protein related to the chromosome condensation regulator RCC1, stimulates guanine nucleotide exchange on ARF1 and Rab proteins. *EMBO J.* **15,** 4262–4273
39. Chong-Kopera, H., Inoki, K., Li, Y., Zhu, T., Garcia-Gonzalo, F. R., Rosa, J. L., and Guan, K. L. (2006) TSC1 stabilizes TSC2 by inhibiting the interaction between TSC2 and the HERC1 ubiquitin ligase. *J. Biol. Chem.* **281,** 8313–8316
40. Costa-Mattioli, M., Sossin, W. S., Klann, E., and Sonenberg, N. (2009) Translational control of long-lasting synaptic plasticity and memory. *Neuron* **61,** 10–26
41. Hoeffer, C. A., and Klann, E. (2010) mTOR signaling: at the crossroads of plasticity, memory, and disease. *Trends Neurosci.* **33,** 67–75
42. Ey, E., Leblond, C. S., and Bourgeron, T. (2011) Behavioral profiles of mouse models for autism spectrum disorders. *Autism Res.* **4,** 5–16